Tuning UWB signals by pulse shaping: Towards context-aware wireless networks

Maria-Gabriella Di Benedetto*, Luca De Nardis

School of Engineering, Infocom Department, University of Rome La Sapienza, Via Eudossiana, 18 – 00184 Rome, Italy

Abstract

Tuning spectra by pulse shaping is feasible in both impulse radio (IR) and continuous radio transmissions, since, as well known, the impulse response of the pulse shaper affects the spectral properties of radiated signals. What is peculiar to IR-UWB, and makes pulse shaping particularly appealing, is the impulsive nature of the carrier. Given their very short duration, transmitted pulses in different intervals overlap neither on clock beats nor in between two clock beats. Spectrum matching in IR can thus be restricted with reasonable approximation to a single inter-pulse interval, and as such be redirected in a rather straightforward way into a waveform representation problem.

This paper analyzes the above problem of tuning radiated IR-UWB signals to reference spectral patterns by pulse shaping, and shows the correspondence between spectrum and waveform matching problems. Examples of application include three case studies: matching the FCC emission masks, mitigating interference in the ISM bands, and reducing inter-system interference for two coexisting UWB networks. The proposed approach goes beyond the signal processing analysis to tentatively propose a procedure and related protocol for integrating spectral adaptation mechanisms into network operating principles.

© 2006 Elsevier B.V. All rights reserved.

Keywords: Context-aware; UWB; Spectral shaping; Impulse radio

1. Introduction

Given their ultra wide bandwidth, ultra wide band (UWB) radio signals must in principle coexist with other radio signals. The problem of possible interference from and onto other communication systems that must be contained within regulated values is thus intrinsic to the UWB radio principle. As such, UWB regulation by the Federal Communications Commission in the United States has opened the way to the concept in large of context-aware radio based on coexistence [1]. This principle fully fits with the emerging innovative concept of "cognitive radio" aimed at defining and developing technologies that can enable a radio device to adapt its spectrum according to the operating environment, that is, to be aware of the scenario in which it operates. The final goal remains to form wireless networks that cooperatively coexist with other wireless networks and devices.

Within this framework, an ambitious goal is the design and development of smart UWB devices able

*Corresponding author. Fax: +39 06 487 33 00.
E-mail addresses: dibenedetto@newyork.ing.uniroma1.it
(M.-G. Di Benedetto), lucadn@newyork.ing.uniroma1.it
(L. De Nardis).

to adapt to the environment, whether this refers to channel or interference patterns, by changing the spectral shape and features of the radiated signals while maintaining compatibility with regulations on emitted radiations.

The UWB signal format offers the interesting and appealing property of being characterized by a high number of tuneable parameters. This is particularly true of impulse radio (IR) UWB signals [2]. This way of forming an UWB signal consists in radiating pulses that are very short in time. The way by which the information data symbols modulate the pulses may vary; pulse position modulation (PPM) and pulse amplitude modulation (PAM) are commonly adopted modulation schemes [3,4]. In addition to modulation and in order to shape the spectrum of the generated signal, the data symbols are encoded by typically using pseudorandom or pseudonoise (PN) codes. In addition, in the case of multi-user communications different codes are assigned to different users in order to limit multi user interference (MUI). In a common approach, the encoded data symbols introduce a time dither on generated pulses leading to time-hopping (TH) coded transmissions. Direct-sequence (DS) encoding is also a viable way. Recent proposals in the United States refer to the DS-UWB alternative [5].

Most important to our goal is the flexibility by which the power spectral density (PSD) of such IR-UWB signals can be modified. Signal features may be appropriately tuned by playing with a variety of parameters. These include transmission factors such as the number of pulses representing one bit, coding factors such as periodicity and cardinality of TH and DS codes, modulation factors related for example to the PPM shift, and shape factors related to specific pulse shapes.

Shaping the spectrum by modifying the pulse waveform is a possibility for both IR and non-IR, i.e. continuous transmissions; it is well known in fact that the impulse response of the pulse shaper affects the PSD of transmitted signals. In IR-UWB, in particular, the envelope of the ultra wide spectrum has a direct correspondence with the transfer function of the pulse shaper [6]. Pulse shaping in IR-UWB has received increasing interest since the release of FCC regulations on UWB emissions [7–11].

What is peculiar to IR-UWB, and makes pulse shaping particularly appealing, is the impulsive nature of the carrier, and, as a consequence, the intrinsic absence of inter-pulse interference, at least

in the transmitted signal. Thanks to their very short duration, transmitted pulses of different pulse intervals will in fact never overlap. In the case of continuous carriers, such as sinusoidal waveforms, satisfying the Nyquist condition guarantees the absence of interference at data clock beats, but does not obviously avoid overlapping of waveforms in between two clock beats. The analysis of PSD matching in the IR case can be thus focused within one inter-pulse interval, and as such be redirected in a rather straightforward way to the problem of matching a target waveform, that is to a waveform representation problem.

This paper addresses the issue of tuning spectral properties of radiated IR-UWB signals to reference spectral patterns by pulse shaping, and analyzes the correspondence between spectrum matching and waveform fitting problems. For this purpose, we first introduce in Section 2 the signal format and related PSD, with particular reference, for conciseness purposes, to TH-PPM modulated signals. Other modulation and coding patterns such as PAM or DS would fit our purpose as long as pulsed transmissions were considered. Section 2 will serve as the basis for Sections 3 and 4 where we discuss possible basic pulse shapes as well as algorithms for solving the spectrum fitting problem. Examples of application of such methods are included in Section 5.

The proposed approach goes beyond the signal processing analysis to tentatively propose a procedure and related protocol for integrating the spectral adaptation mechanism into network operating principles, as will be discussed in Section 6. Section 7 draws the conclusions and sets guidelines for future work.

2. Time-hopping impulse radio PPM ultra wide band signal format and related power spectral density

The signal format adopted in this paper refers to sequences of pulses that are modulated in position by the source data in a TH-PPM fashion. As mentioned in the Introduction, limiting the analysis to TH-PPM does not imply a loss of generality, since other modulation and coding strategies such as PAM or DS would fit our purpose as long as pulsed transmissions were considered.

Suppose that binary data flows originate from N_u users with same bit rate $R_b = 1/T_b$, where T_b is the bit period. In order to avoid catastrophic collisions, each user is associated with a different TH code.

The transmitted signal by the nth user can be expressed as follows:

$$s_{TX}^{(n)}(t) = \sum_{j=-\infty}^{\infty} p(t - jT_s - c_j^{(n)}T_c - \varepsilon d_j^{(n)}), \qquad (1)$$

where $p(t)$ is the impulse response of the pulse shaper. According to Eq. (1), the UWB signal consists of a train of pulses that are transmitted with an average repetition time T_s. The jth pulse is further shifted by two additional amounts due to coding and modulation, as will be described below.

The $c_j^{(n)}T_c$ term represents the effect of the TH code, where $c_j^{(n)}$ is the jth coefficient of the TH sequence assigned to the nth user and T_c is the basic time-shift introduced by the TH code that is the chip time. A TH code is formed by a sequence of N_p independent and identically distributed random variables, all characterized by a probability $1/N_h$ to assume one of the integer values in the range $[0, N_h - 1]$. Each TH code has same probability of being selected and is independent of all other codes.

The $\varepsilon d_j^{(n)}$ term represents the time-shift which is eventually introduced by the modulation, where ε is the PPM dither and $d_j^{(n)}$ is the binary value conveyed by the jth pulse. In principle, one single pulse may be used to represent one bit. In order to improve system robustness, however, it is common sense to use more than one pulse for representing a bit. In the general case of N_s pulses per bit, the PPM scheme operates by shifting all N_s pulses corresponding to a 1-bit by ε. The signal format in Eq. (1) thus rewrites

$$s_{TX}^{(n)}(t) = \sum_{j=-\infty}^{\infty} p(t - jT_s - c_j^{(n)}T_c - \varepsilon b_{\lfloor j/N_s \rfloor}^{(n)}), \qquad (2)$$

where $\lfloor x \rfloor$ is the inferior integer part of x and $b_x^{(n)} = b^{(n)}(xT_b)$ is the xth bit of the binary data flow of user n. We assume that all bits are independent and identically distributed random variables with equal probability of being 0 or 1.

In order to avoid both pulse overlapping and ambiguity between pulse positions, a few constraints must be introduced among signal parameters of Eq. (2), such as $T_s \leqslant T_b/N_s$, $T_c \leqslant T_s/N_h$ and $\varepsilon \leqslant T_c - T_M$ where T_M represents the time duration of the single pulse $p(t)$.

The PSD of a TH-PPM signal can be found in a rather straightforward way for the common case $N_p = N_s$ [2]. Consider a multi-pulse signal $y(t)$ defined as follows:

$$y(t) = \sum_{j=1}^{N_s} p(t - jT_s - c_j^{(n)}T_c). \qquad (3)$$

The Fourier transform of the above signal is

$$P_y(f) = P(f) \sum_{m=1}^{N_s} e^{-j(2\pi f(mT_s + \eta_m))}, \qquad (4)$$

where η is the cumulative time-shift due to modulation and coding.

If we now consider $y(t)$ as the basic multi-pulse used for transmission and apply the ε PPM shift, we obtain the following expression for the transmitted signal:

$$s(t) = \sum_{j=-\infty}^{+\infty} y(t - jT_b - \varepsilon b_j), \qquad (5)$$

that is a PPM modulated waveform in which the shift is ruled by the sequence of source data symbols $\mathbf{b}$. Assuming that $\mathbf{b}$ is a strict-sense stationary discrete random process, and that the different extracted random variables b_k are statistically independent with a common probability density function w, the following spectrum of a TH-IR-PPM signal is obtained:

$$P_s(f) = \frac{|P_y(f)|^2}{T_b} \left[1 - |W(f)|^2 \right.$$
$$\left. + \frac{|W(f)|^2}{T_b} \sum_{n=-\infty}^{+\infty} \delta\left(f - \frac{n}{T_b} \right) \right]. \qquad (6)$$

Eq. (6) shows the double effect of the TH code through $P_y(f)$, and of the time shift introduced by PPM with behavior following the statistical properties of the source represented by $|W(f)|^2$. Note that the discrete component of the spectrum has lines with amplitude weighted by $|W(f)|^2$, located at multiples of $1/T_b$. If p indicates the probability of emitting a "0" bit (no shift) and $1-p$ the probability of emitting a "1" bit (ε shift), one can write $|W(f)|^2 = 1 + 2p^2(1 - \cos(2\pi f \varepsilon)) - 2p(1 - \cos(2\pi f \varepsilon))$ and if $p = \frac{1}{2}$, then $|W(f)|^2 = \frac{1}{2}(1 + \cos(2\pi f \varepsilon))$.

From Eq. (6), since both the continuous and discrete components of the PSD are shaped by $|P(f)|^2$, we may approximate the PSD of radiated TH-PPM signals by $|P(f)|^2$. Given the impulse nature of the transmission we will then be able to confine the analysis to one single pulse interval T_s, as will be shown in Section 4.2.

3. Reference pulses in UWB

The reference pulse in UWB communications is often called monocycle that is one cycle of a pulse-modulated sine wave as typical of conventional radar applications, although in effect it is rarely a cycle of a sine wave. Non-sinusoidal pulses are in fact less difficult and expensive to generate than pulse-modulated sine waves. Generating pulses of duration on the order of a nanosecond with an inexpensive technology (CMOS chips) has become possible after UWB large current radiator (LCR) antennas were introduced by Harmuth [12]. The LCR antenna is driven by a current; the antenna radiates a power that is proportional to the square of the derivative of the current. When a step current is applied to the antenna, a pulse is generated: The steeper the step, the narrower the generated pulse [13].

The easiest pulse shape to generate by a pulse generator has a bell shape such as the Gaussian pulse $p_G(t)$, where $p_G(t)$ can be assumed to be a voltage waveform and is given by:

$$p_G(t) = \pm \frac{1}{\sqrt{2\pi\sigma^2}} e^{-(t^2/2\sigma^2)} = \pm \frac{\sqrt{2}}{\alpha} e^{-2\pi t^2/\alpha^2}, \qquad (7)$$

where $\alpha^2 = 4\pi\sigma^2$ indicates the shape factor and σ^2 the variance.

The voltage waveform of Eq. (7) is plotted in Fig. 1(a). It is an energy signal, that is it has finite energy. The corresponding energy spectral density (ESD) of the pulse of Eq. (7) is shown in Fig. 1(b). Since we assume that $p_G(t)$ is a voltage, its total energy is expressed in V^2s and its ESD is in V^2s/Hz.

The reference Gaussian pulse of Fig. 1 does not comply, however, with a basic feature that can guarantee its efficient radiation, that is, to have a zero dc (direct current) offset. To this respect, Gaussian derivatives might be suitable, and as a matter of fact the second Gaussian derivative is one of the most commonly selected pulse [14]. It is described by:

$$\frac{d^2 p_G(t)}{dt^2} = \left(1 - 4\pi \frac{t^2}{\alpha^2}\right) e^{-2\pi t^2/\alpha^2}, \qquad (8)$$

with energy $3\alpha/8\ V^2$s. Other basic pulse waveforms have been proposed such as the Laplacian [15] and Hermite pulses [7].

The second Gaussian derivative pulse defined in Eq. (8) is commonly referred to as the pulse at the receiver, that is after passing through the transmitter and receiver antennas. Ideally, a second derivative Gaussian pulse can be obtained at the output of the transmitting antenna if the antenna is fed with a current pulse shaped as the first derivative of a Gaussian waveform (and thus zero dc current), the radiating pulse being proportional to the derivative of the drive current in an ideal antenna [16]. One should note that for the reciprocity theorem, the behavior of the receiving antenna should not be assimilated to the transmitter one. In particular, when receiving, the antenna does not act as a derivator on the incoming signal, but rather presents a flat frequency response [17].

One should note, however, that for our purposes the shape of both the radiated and received pulses should be considered. The first condition is imposed by compliance with emission masks while the second should take into account operating
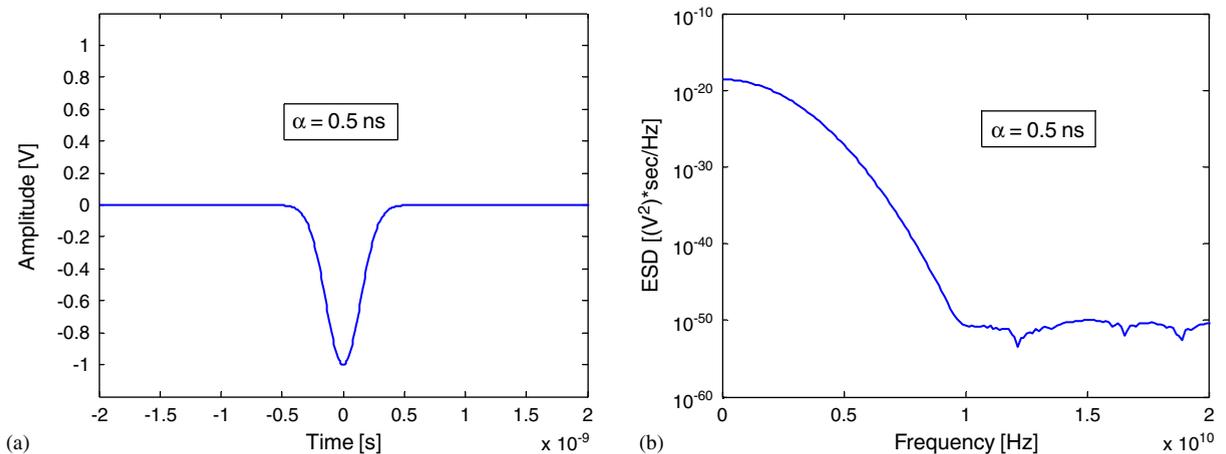

Fig. 1. Example of a Gaussian pulse: (left) voltage waveform, and (right) corresponding ESD.

conditions at the receiver and in particular channel as well as MUI characteristics.

4. Adjusting emitted radiations to context

In this section, we analyze the problem of adjusting emitted radiations to context. In particular, we are interested in defining an automatic procedure for tuning an emitted signal in order to approximate a pre-defined target spectral pattern.

The target spectral pattern may derive from different system requirements. A high-priority requirement refers to emission masks set by regulation authorities. The effort should focus in this case on using power at best, while keeping compliance with regulation.

In addition, requirements may be posed by channel characteristics. Channel constraints may include not only the transmission medium but also effects introduced by the presence of multiple users belonging to either autochthon or foreign networks. In this section, we focus on the algorithm that implements the optimization procedure relative to spectrum tuning. The problem of conceiving a protocol that allows the application of the above procedure within a context-aware network formed by several users and communication links will be the object of Section 6.

In order to build up the procedure, Section 4.1 first defines a target PSD mask. The optimization algorithm suitable to our goal is then presented in Section 4.2.

4.1. Reading an emission mask

In order to understand how to read an emission mask, it is necessary to define the effective isotropic radiated power (EIRP) for a given range of operating frequencies. EIRP is given by the product of the available power of the transmitter W_{TX}, expressed in watts, i.e. the maximum power that the transmitter can transfer to the transmitter antenna, and the gain of the transmitter antenna G_{AT}, that is EIRP $= W_{TX}G_{AT}$. The available power of the transmitter W_{TX} is effectively transferred from the transmitter to the antenna when the condition for maximum power transfer between the output impedance of the transmitter Z_{oTX} and input impedance of the antenna Z_{AT} is verified, that is $Z_{AT} = Z_{oTX*}$ EIRP is usually measured in dBm that is as $10\log_{10}\text{EIRP}_{\text{mWatts}}$. Note that for isotropic antennas, as most common for nodes of ad hoc

networks and as will be assumed below, $G_{AT} = 1$ and thus EIRP $= W_{TX}$. We will indicate by "W_{TX}" radiated power, expressed in watts, oppositely to signal power "P_{TX}", expressed in (volts)^2.

An equivalent way of ruling emitted radiations is to impose limits on the field strength V_s. The field strength represents the voltage one should apply to an impedance equal to the characteristic impedance of free-space Z_{FS} to obtain a radiated power W_{TX} after propagation over a distance D. Z_{FS} is related to permeability and permittivity of free space and is equal to approximately $377\,\Omega$ (the exact value being 120π). In principle, Z_{FS} is independent of frequency. The relation between field strength (expressed in V/m) and radiated power is thus

$$W_{TX} \cong \frac{V_s^2}{377} 4\pi D^2. \tag{9}$$

The power defined by Eq. (9) is an average radiated power. In a binary IR scheme, the average power of the signal is computed by averaging the energy of the N_s pulses representing one bit over the bit interval T_b, or equivalently averaging the energy of one pulse over the pulse interval T_s. Given the energy of a single pulse, E_p (in V^{2}s), and the total energy of the pulses representing one bit, N_sE_p, the average power P_{av} (in V^2) under the hypothesis $T_b = N_sT_s$ is thus expressed by

$$P_{av} = \frac{N_sE_p}{T_b} = \frac{N_sE_p}{N_sT_s} = \frac{E_p}{T_s}, \tag{10}$$

where $1/T_s$ is the pulse repetition rate. Different signals can thus have same P_{av} with different pulse energy values E_p, depending on $1/T_s$. At equal average power, signals with low repetition rate may have higher E_p. For equal pulse duration, this is equivalent to saying that the maximum instantaneous power may be markedly different among signals with similar average power.

Emission masks typically impose limits on the PSD of emitted signals that is on *radiated* PSD, expressed, for example, in dBm/Hz or dBm/MHz. Emission masks are, however, commonly provided in practice in terms of power values at a given frequency, rather than power density values. The value of the emission mask at a given frequency f_c indicates, in fact, the maximum allowed radiated power within a measured bandwidth (mb) centered around f_c. Such a power value, denoted as W_{mb}, coincides with the radiated power of a transmitted signal W_{TX} only when the bandwidth B of the transmitted signal is equal to the measured bandwidth mb. The measured bandwidth

mb reflects thus the resolution of the measurement tools in use. For a signal occupying a bandwidth greater than mb, the maximum allowed total radiated power W_{TX} is equal to the sum of the W_{mb} values that are provided by the mask corresponding to the frequency range occupied by the signal. In the particular case where the W_{mb} value indicated by the mask is constant over B, one has

$$W_{mb}\frac{B}{mb} = W_{TX} \simeq \frac{V^2}{377}4\pi D^2. \tag{11}$$

Note that Eq. (11) provides a formal definition of W_{mb} as the maximum allowed W_{TX} for a signal having $B = mb$.

Consider for example the FCC emission regulation for UWB [1]. Besides power values for a 1 MHz measured bandwidth as shown in the masks, the rules also specify a limit on the peak level of emission within a 50 MHz bandwidth centered on frequency f_M at which the highest radiated emission occurs. The limit is set to 0 dBm/50 MHz, that is, the power computed over a frequency range of 50 MHz around f_M is limited to 0 dBm.

4.2. Matching a target mask

In this paragraph, we present an analytical approach to the problem of finding a best match between reference and radiated spectral patterns. The proposed approach leads to an approximation of the reference pattern by linear combination of N independent base functions (BF) in a space of N dimensions. The choice of the coefficients of the linear combination must be made depending upon a design objective by defining a distance between the target and approximating function. We will show in this section how to redirect the problem of spectral matching onto a problem of waveform representation.

Let us first consider the problem in the time domain. Indicate by $v(t)$ a target function, that is in our analysis a field strength or target voltage, and by $\phi_k(t)$ the BFs, with $k = 1, \ldots, N$. One way of selecting the linear combination coefficients a_k is to apply a standard procedure such as the least square error (LSE). In this case, the aim is to minimize a distance between target and linear combination, which is defined as follows:

$$e_v = \int_{-\infty}^{+\infty} |e(t)|^2 \, dt = \int_{-\infty}^{+\infty} \left| v(t) - \sum_{k=1}^{N} a_k \phi_k(t) \right|^2 \, dt. \tag{12}$$

Note, however, that commonly the target function is specified in terms of a radiated power spectrum. We need then to define a spectral distance between reference and approximating patterns. The error to be minimized can in this case be expressed as follows:

$$e_W = \int_{-\infty}^{+\infty} |W_v(f) - W_\phi(f)|^2 \, df, \tag{13}$$

where $W_v(f)$ represents the target radiated PSD and $W_\phi(f)$ a corresponding radiated PSD of the linear combination, both expressed in watts/Hz that is in $V^2/(\text{ohms Hz})$. Since both powers are radiated over the same impedance Z_{FS}, one can write equivalently to Eq. (13):

$$e_P = \int_{-\infty}^{+\infty} |W_v(f)Z_{FS} - W_\phi(f)Z_{FS}|^2 \, df$$
$$= \int_{-\infty}^{+\infty} |P_v(f) - P_\phi(f)|^2 \, df, \tag{14}$$

where $P_v(f)$ represents the target signal PSD and $P_\phi(f)$ a corresponding signal PSD of the linear combination, both expressed in V^2/Hz. Equivalently to Eq. (13), one can consider the autocorrelation functions $R_v(t)$ and $R_\phi(t)$ and minimize the following distance:

$$e_R = \int_{-\infty}^{+\infty} |R_v(t) - R_\phi(t)|^2 \, dt$$
$$= \int_{-\infty}^{+\infty} \left| R_v(t) - \left[\sum_{k=1}^{N} a_k^2 \int_{-\infty}^{+\infty} \phi_k(\xi) \right.\right.$$
$$\left.\left. \times \phi_k^*(\xi + t) \, d\xi \right] \right|^2 \, dt. \tag{15}$$

Eqs. (13)–(15) can be reconciled with Eq. (12); in the IR case, the target signal is an energy signal such as a pulse defined over a time interval T_s with an ESD that can be derived by normalizing the signal PSD by $1/T_s$. Take for example Eq. (13); The target emission voltage $v(t)$ can be obtained by dividing the target radiated PSD, normalized by $1/T_s$, by the free space impedance, taking the square root, and applying the Fourier anti-transform. One obtains thus

$$v(t) = F^{-1}\left(\sqrt{W_v(f)Z_{FS}T_s} \right), \tag{16}$$

and the minimization function is defined by Eq. (12). Eq. (16) can be illustrated on the basis of the FCC UWB indoor emission masks [1] shown Fig. 2(a). Fig. 2(b) shows the emission voltage
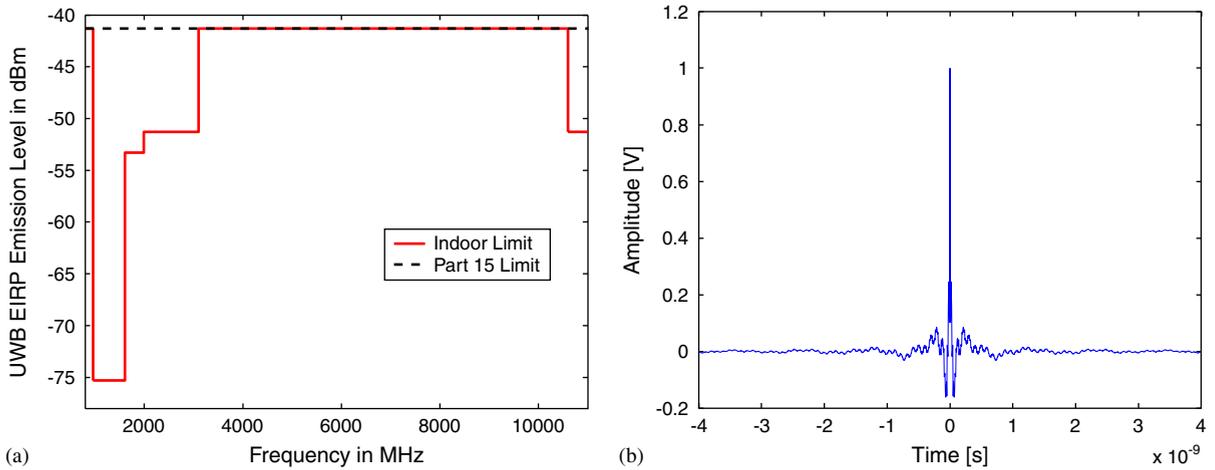
Fig. 2. FCC indoor emission mask for UWB devices [1] (a), and corresponding amplitude-normalized voltage waveform (b). The pulse of (b) satisfies Eq. (16) and has a radiated PSD as of (a).

obtained by applying Eq. (16) that is the pulse of Fig. 2(b) has spectral properties as of Fig. 2(a). Matching the spectrum of Fig. 2(a) can be thus redirected into matching the waveform of Fig. 2(b), as expressed by Eq. (12).

As a first remark, note that the LSE optimization procedure is based on an average quadratic distance and as such it does not imply bounds on a frequency-by-frequency basis. In the case of absence of frequency-dependent constraints, the above optimization procedure leads to admissible solutions. When frequency-dependent bounds are imposed such as in the case of masks defined by regulatory bodies, it is necessary to introduce in the definition of the minimization problem the bounds set by the target mask. In summary, the problem that needs to be solved is:

$$\min_{a_k} \left\{ e_v = \int_{-\infty}^{+\infty} \left| v(t) - \sum_{k=1}^{N} a_k \phi_k(t) \right|^2 dt \right\} \quad (17)$$

with

$$W_\phi(f) < W_v(f).$$

The second comment refers to measurement tools as indicated in Section 4.1, and related resolution. If one takes into account the measured bandwidth, the minimization problem of Eq. (17) can be expressed in a straightforward way by imposing a discrete form of the bound, that states as follows:

$$\min_{a_k} \left\{ e_v = \int_{-\infty}^{+\infty} \left| v(t) - \sum_{k=1}^{N} a_k \phi_k(t) \right|^2 dt \right\}$$

with

$$W_{d\phi}(k) < W_{dv}(k) \quad \text{for } k = 0, \dots, +\infty, \quad (18)$$

where

$$W_{d\phi}(k) = \frac{1}{\text{mb}} \int_{k \cdot \text{mb}}^{(k+1)\text{mb}} W_\phi(f) \, df$$

and

$$W_{dv}(k) = \frac{1}{\text{mb}} \int_{k \cdot \text{mb}}^{(k+1)\text{mb}} W_v(f) \, df.$$

Note that when solving the above problem by means of simulation tools, a measured bandwidth is implicitly assumed as soon as the distance between two samples of a given function in the frequency domain is set equal to the measured bandwidth.

5. Pulse shaping: case studies

In this section, application of the algorithms proposed in Section 4.2 is presented for three case studies. In all cases, the first N derivatives of the Gaussian pulse are adopted as BFs. The choice of analyzing the Gaussian derivatives case naturally derives from the large use of these functions in UWB current literature. Each derivative is characterized by a given α value (different derivatives may have different α values).

The first case study analyzes the problem of approximating the FCC emission mask for indoor UWB devices (see Fig. 2(a)); the goal in this case is to obtain a radiated PSD at the transmitter as close as possible to the FCC spectral mask, while satisfying the upper bound set in Eq. (18).

The second case study considers the problem of mitigating the interference created by narrowband transmissions at an UWB receiver; the goal is to obtain a radiated PSD at the receiver that avoids the frequency intervals used by the narrowband transmissions.

Finally, in the third case study, we analyze the problem of mitigating mutual interference between overlapping IR-UWB networks, by selecting different pulse shapes for the different UWB networks.

5.1. Approximation of FCC spectral masks

In this section we will address the problem of finding a pulse waveform that approximates the FCC emission masks at all frequencies, including the 0–0.96 GHz band. The problem of meeting the FCC emission masks for UWB emissions by pulse shaping has already been addressed in the past, mainly focusing on frequencies above 3.1 GHz [18–21].

Application of the LSE method presented in the previous section led to the black continuous curve in Fig. 3, when considering a BF set formed by the first 15 Gaussian derivatives with $\alpha = 0.714$ ns for all derivatives.

Note the occasional violation of the mask of the continuous plot in Fig. 3. Obtaining a waveform fully compliant with the upper bound of Eq. (18) requires either achieving an error-free waveform matching, or converting the upper bound into a form that can be taken into account in the approximation procedure performed in the time domain.

A possible empirical approach to the problem is to select the coefficients of the linear combination by means of a computer-based trial-and-error loop according to a procedure that can be described as follows:

1. Choose a set of BFs.
2. Generate in a random way a set of coefficients, named S.
3. Check if the PSD of the linear combination of the functions obtained with coefficients S satisfies the emission limits. Note that this check should be done based on the measurement bandwidth as defined in the previous subsection.
4. If the emission limits in Step 3 are met and this is the first set S verifying the limits, then initialize the procedure by setting $SB = S$. If the emission limits in Step 3 are met and the procedure was already initialized, then compare S with SB; if S
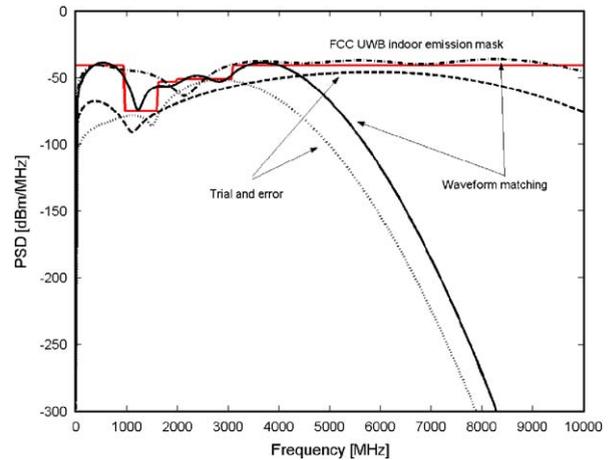

Fig. 3. PSD of the linear combination of the first 15 Gaussian derivatives vs. FCC indoor emission mask. The black continuous curve represents the matching that is found with the LSE method with $\alpha = 0.714$ ns for all derivatives. The upper dashed and dotted curve represents the matching that is found with the LSE method with $\alpha = 1.5$ ns for the first derivative and $\alpha = 0.314$ ns for higher derivatives. The remaining two non-continuous curves are obtained by using a trial-and-error procedure. Dotted curve: $\alpha = 0.714$ ns for all derivatives, and dashed curve: $\alpha = 1.5$ ns for the first derivative and $\alpha = 0.314$ ns for higher derivatives.

leads to a better waveform than SB according to well-defined distance metrics, set $SB = S$.
5. Repeat Steps 1–3 until the distance between the mask and PSD of the generated waveform falls below a fixed threshold.

Note that the combination of N derivatives provides a high degree of flexibility in the generation of pulse waveforms. Compliance with the upper bound of Eq. (18) is directly checked during the selection procedure, and non-admissible solutions are discarded. The algorithm may, however, require a high number of iterations before converging.

The PSD of a waveform obtained by using the trial-and-error procedure using the 15 Gaussian derivatives with α values all equal to 0.714 ns is shown in Fig. 3 (dotted curve), showing a good approximation in the band 0.96–3.6 GHz, while outside this band power is not efficiently used. A comparison of the continuous (waveform matching) vs. dotted (trial-and-error) curves of Fig. 3 shows that compliance with mask guaranteed by the trial-and-error procedure is obtained at the price of a reduced efficiency.

Improved performance can be achieved by adopting different α values for the different derivatives. Consider a second set of α values characterized by a higher value

of α (1.5 ns) for the first derivative and smaller values (0.314 ns) for the other derivatives. Applying waveform matching leads to the PSD represented by the upper curve (dashed-dotted curve of Fig. 3). This PSD achieves a better approximation of the mask at higher frequencies than the continuous one, thanks to the larger bandwidth of higher derivatives. Note that this result is achieved at the price of larger violations of the mask at low frequencies.

The new α values also improve performance of the trial-and-error procedure, as shown in Fig. 3 (dashed plot), leading to a PSD that is quite close to the target for frequencies up to about 7.5 GHz. Note that the selection of a relatively high α for the first derivative improves efficiency in power utilization at low frequencies. An upper bound for α is given, however, by waveform duration, as determined by the chip time T_c.

5.2. Mitigation of narrowband interference

In this section, we will show how pulse shaping can be used for mitigating the interference generated by narrowband transmitters on an UWB receiver. Note that, oppositely to Section 5.1, interference mitigation by pulse shaping requires here cooperation between transmitter and receiver, since the transmitted pulse shape must be selected after taking into account interference conditions at the receiver. This aspect will be further discussed in Section 6.

We will focus in particular on narrowband transmitters in the ISM bands reported in Table 1.

In order to protect the UWB link from interfering emissions in the ISM bands, a pulse shape leading to a radiated PSD allocating low power in these bands would be suitable. Let us arbitrarily define a target radiated PSD with power density values in frequency intervals of 500 MHz centered on each of the ISM bands that are 50 dB below the values at other frequencies. Such a mask is shown in Fig. 4(a).

The same procedure of Section 5.1 can be applied. Note, however, that in the present case occasional violations of the target PSD mask may be tolerated,

since the mask was not imposed by regulation. The target waveform corresponding to the target PSD in Fig. 4(a) is shown in 4(b). Application of the LSE method with a BF set formed by the first 15 Gaussian derivatives with $\alpha = 0.714$ ns for all derivatives leads to the results of Fig. 5. Note that the intermediate bandwidth might not be sufficiently well protected, and therefore there might be a need for imposing the upper bound of Eq. (18). Improved results can be obtained by selecting different α values for different derivatives.

5.3. MUI control by pulse shaping

A flexible pulse shaping function can guarantee high robustness towards inter-network interference in overlapping UWB networks by adopting different pulse shapes in the two networks. In UWB networks based on TH-CDMA, MUI is a predominant factor in determining the maximum achievable bit rate, in particular for medium to high rate transmissions. A MAC protocol able to select different pulse shapes may optimize network organization by assigning different pulses to different groups of terminals. This approach was tested for two disjoint UWB networks, N1 and N2, co-located in the same geographical area. Each network was composed of 24 devices transmitting at $R_b = 50$ Mb/s. The effect of interference generated in both N1 and N2 on a useful link of N1 was analyzed by measuring BER vs. E_b/N_0. Pulse shape in N1 was the second Gaussian derivative, while it varied in N2 at each simulation run.

Results are presented in Fig. 6 in the case of second, fourth and eighth derivative of the Gaussian pulse as adopted pulse in N2. Results show that the adoption of different waveforms in the two networks reduces BER, thanks to bandwidths differentiation. This is also confirmed by the fact that higher derivatives adopted in N2 lead to lower BER, due to the effect of differentiation on bandwidth and peak frequency [2]. Note that the strategy of assigning different waveforms to different networks can be applied to linear combinations of BFs as well, in order to guarantee both low interference and good approximation of the emission masks.

6. Protocol design for context-aware wireless networks

In this section, we analyze the problem of integrating the mechanism for spectrum adaptation

Table 1
Frequency occupation of the ISM bands

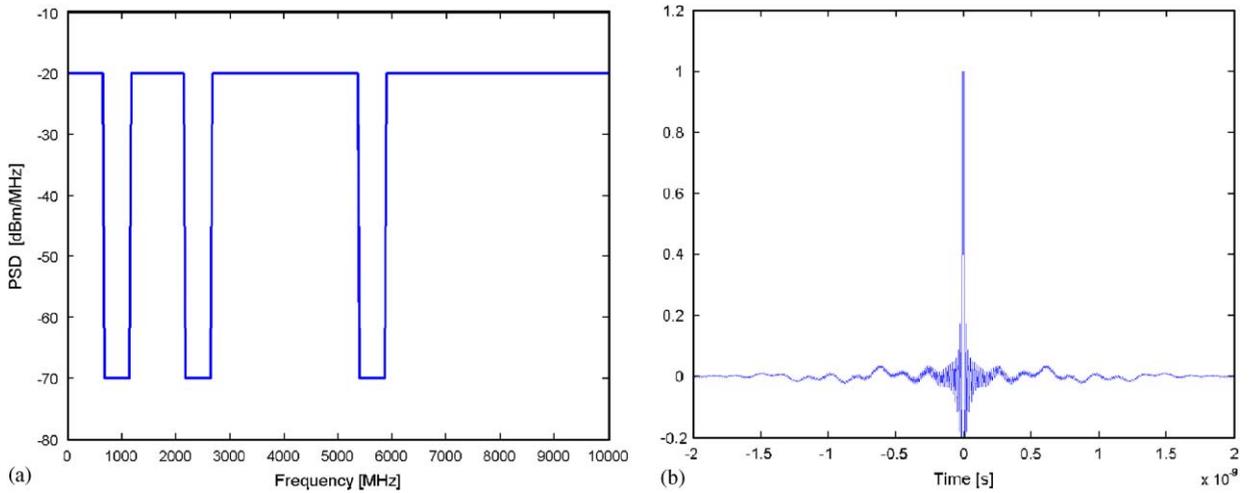| ISM band	Frequency range
I	902–928 MHz (26 MHz)
II	2.4–2.4835 GHz (83.5 MHz)
III	5.725–5.85 GHz (125 MHz)

Fig. 4. Target radiated PSD for mitigation of the effects of narrowband interference in the ISM bands on a UWB receiver (a), and corresponding amplitude-normalized voltage waveform associated with the radiated PSD (b), that is the voltage of (b) has a radiated PSD as of (a).
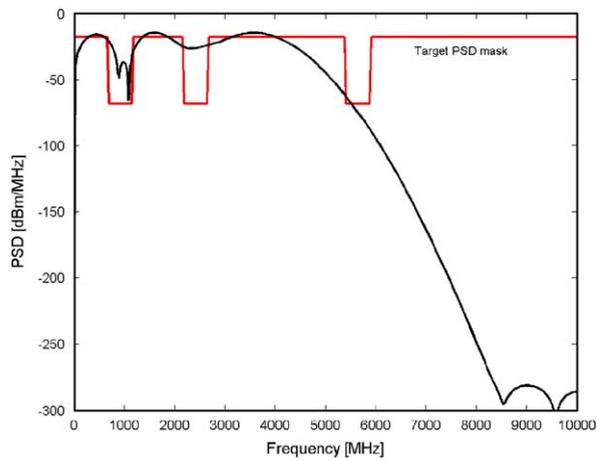

Fig. 5. PSD of the linear combination of Gaussian waveforms obtained by waveform matching with $\alpha = 0.714$ ns for all derivatives vs. target PSD mask.

Fig. 6. BER vs. E_b/N_0 for different adopted pulses in two UWB networks N1 and N2 (Circles: both N1 and N2 use the II Gaussian derivative; Squares: N1 and N2 use the II and IV Gaussian derivative, respectively; Diamonds: N1 and N2 use the II and VIII Gaussian derivative, respectively).

presented in the previous sections into an operational environment. The problem becomes increasingly complex as a function of the complexity and compatibility in the set of constraints imposed by operational conditions.

Let us consider first the rather simple case of a network formed by only two nodes that transmit and receive over one single link. Within this framework, the aim is to identify a pulse shape that satisfies the two following conditions:

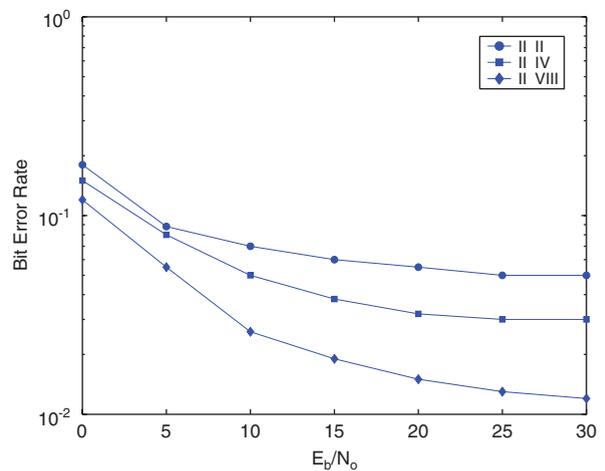1. The radiated PSD must be compliant with emission masks reflecting both regulation and eventually power constraints induced by the presence of coexisting networks.
2. The received radiated PSD must be such that channel impairments are counteracted at best. The pulse shape selection process is in this case dynamic and equivalent to a pre-equalization at the transmitter.

Satisfying the first condition should be a built-in mechanism of a transmitter. In particular, the emission mask at the transmitter must reflect the

constraint imposed by regulation such as the emission masks of Fig. 2(a), but also respect coexistence issues; to this regard possible coexistence with other networks such as WiFi [22], WiMax [23] and networks for example in the ISM band [24] should be taken into account. In Europe coexisting networks, in particular at 900 MHz, include cellular GSM phones [25]. A possible mechanism for spectrum adaptation could be based on the presence in the node of a table or database of possible waveforms that have been previously and once for all determined to be suitable for different scenarios of operation. The transmitter may then select the waveform based on different mechanisms depending upon its complexity. In the case of higher sophistication, the transmitter may be capable of sensing the channel and building a view of the expected performance in terms of signal to noise ratio as a function of frequency SNR(f). The structure of a UWB receiver that can also be used for sensing the channel usually foresees the presence of a correlator followed by an integrator [2]. The evaluation of SNR(f) may be possible if the output of the correlator can be isolated and analyzed before integration. For simpler implementations of the channel sensing mechanism, i.e. based on integrated energy evaluations, the transmitter may evaluate a global SNR and select a pulse waveform according to predetermined rules.

Satisfying the second condition requires information on the environment at the receiver. It is necessary, therefore, to design an exchange procedure that enables a transmitter to be informed by a receiver about current channel configuration. Equivalently, the selection of the pulse waveform may be done by the receiver itself; the information sent by the receiver back to the transmitter might then be in this case limited to an identifier of the pulse waveform to be used. The discussion of the above paragraph regarding the pulse decision process can be duplicated here. The decision process of how to select the pulse depends upon the complexity of the receiver. In particular, for simple channel sensing mechanisms, the pulse might be selected from a database of possible pulses that is shared by all nodes, each pulse being identified by a code in the database. This mechanism would basically resemble the one described in the previous paragraph.

Since both conditions should be verified at once, the mechanism based on the creation of a look-up table of pulses has the advantage of allowing

convergence as well as of being relatively simple. Common sense suggests that this selection should take place at the receiver provided that the transmitter has communicated to the receiver all the constraints to be met by the first condition.

Let us move to the more complex case of a network of several nodes with several active links between nodes. Here, pulse selection must also include MUI mitigation considerations. Again, as for channel impairment issues, the context adaptation mechanism should take into account MUI characteristics at the receiver. In this case, it is necessary to implement a MAC module including a hand-shake mechanism in order to allow link set-up and information exchange between transmitter and receiver regarding which pulse to be used for meeting requirements at both transmitter and receiver. Note that simultaneous execution of the selection procedure over independent links could lead to network instability. This problem is common to all distributed approaches in ad hoc networks, as for example in the distributed power-control problem [26]. To this regard, the mechanism suggested in the previous paragraphs of building up a database of pulses from which selecting the most suitable pulse has the advantage of being simple and guarantee convergence.

7. Conclusions and future work

IR-UWB signals are characterized by an interesting feature; their spectral properties may be appropriately tuned by playing with a variety of parameters. In this paper, we analyzed the issue of tuning spectral properties of radiated IR-UWB signals to reference spectral patterns by pulse shaping. We showed that the impulsive nature of the carrier of IR allows translating the problem of matching a spectrum, into the problem of finding a best waveform match. We proposed a method for obtaining the approximating function based on the minimization of the squared distance between target and a synthetic waveform obtained by linear combination of a set a pre-defined BFs.

Results obtained by application of the proposed algorithm were presented for three case studies. In the three cases, the set of BFs was formed by the first N derivatives of the Gaussian pulse. The first case study refers to approximating FCC indoor UWB emission masks. The best fitting curve was compared to a fit that can be found by using a pure trial-and-error method. A similar analysis was

carried out in a second case study that analyzed the problem of preventing possible interference on a UWB network from coexisting networks operating in the ISM bands. Finally, in the third case study, we addressed the issue of reducing interference noise generated by a coexisting and foreign UWB network onto a UWB network. A good spectrum matching was obtained, especially in the case of no frequency-by-frequency spectrum upper bounds. Finally, we proposed a procedure and related protocol for integrating the spectral adaptation mechanism into network operating principles.

The above results should be considered as a first step in the definition of algorithms and procedures aimed at setting the basis for the design of context-aware UWB networks. Our view of future investigations includes integrating the bounds in the minimization function and testing the procedure using traditional optimization methods. Non-linear optimization is also an interesting area of development. Of a high priority is also the possibility of tuning UWB spectral properties by controlling properties of the codes. In the case of TH-PPM signals, this is not an easy task since the effect of TH code properties vs. modulation effects is not easily determined [27]. Last but not least, the MAC protocol allowing implementation of the tuning procedure will be fully designed and tested.

Acknowledgment

References

[1] Federal Communications Commission, Revision of part 15 of the Commission's rules regarding ultra-wideband transmission systems: first report and order, Technical Report FCC 02-48 (adopted February 14, 2002; released April 22, 2002).

[2] M.-G. Di Benedetto, G. Giancola, Understanding Ultra Wide Band Radio Fundamentals, Prentice-Hall Pearson Education, Inc., Upper Saddle River, New Jersey, 2004.

[3] M.L. Welborn, System considerations for ultrawideband wireless networks, IEEE Radio and Wireless Conference, August 2001, pp. 5–8.

[4] I. Guvenc, H. Arslan, On the modulation options for UWB Systems, IEEE Military Communications Conference, October 2003, pp. 892–897.

[5] R. Fisher, R. Kohno, H. Ogawa, H. Zhang, K. Takizawa, M.Mc Laughlin, M. Welborn, DS-UWB Physical Layer

Submission to 802.15 Task Group 3a. Available at ⟨ftp://ieee:wireless@ftp.802wirelessworld.com/15/04/15-04-0137-03-003a-merger2-proposal-ds-uwb-update⟩, July 2004.

[6] M.-G. Di Benedetto, B.R. Vojcic, Ultra wide band (UWB) wireless communications: a tutorial (Special Issue on Ultra-Wideband Communications), J. Comm. Networks 5 (4) (2003) 290–302.

[7] M. Ghavami, L.B. Michael, S. Haruyama, R. Kohno, A novel UWB pulse shape modulation system, Wireless Personal Comm. 23 (1) (2002) 105–120.

[8] L.B. Michael, M. Ghavami, R. Kohno, Multiple pulse generator for ultra-wideband communication using Hermite polynomial based orthogonal pulses, IEEE Ultra Wideband Systems and Technologies, Baltimore MA, May 2002, pp. 47–51.

[9] G.T.F. de Abreu, R. Kohno, Design of Jitter-robust orthogonal pulses for UWB systems, IEEE Global Telecommunications Conference, December 2003, pp. 739–743.

[10] G.T.F. de Abreu, G.J. Mitchell, R. Kohno, On the design of orthogonal pulse-shape modulation for UWB systems using Hermite pulses (Special Issue on Ultra-Wideband Communications), J. Comm. Networks 5 (4) (2003) 328–343.

[11] D. Zeng, A. Annamalai Jr., A.I. Zaghloul, Pulse shaping filter design in UWB system, IEEE Conference on Ultra Wideband Systems and Technologies, Reston, VA, November 2003, pp. 66–70.

[12] H.F. Harmuth, Radiation of Nonsinusoidal Electromagnetic Waves, Academic Press, New York, 1990.

[13] A.F. Kardo-Sysoev, Generation and radiation of UWB signals, International Workshop on Ultra Wideband Systems, Oulu, Finland, June 2003.

[14] M.Z. Win, R.A. Scholtz, Ultra-wide bandwidth time-hopping spread-spectrum impulse radio for wireless multiple-access communications, IEEE Trans. Comm. 48 (4) (2000) 679–691.

[15] J.T. Conroy, J.L. LoCicero, D.R. Ucci, Communication techniques using monopulse waveforms, IEEE Military Communications Conference Proceedings, vol. 2, November 1999, pp. 1181–1185.

[16] I.I. Immoreev, N. Sinyavin, Features of ultra-wideband signals' radiation, IEEE Conference on Ultra Wideband Systems and Technologies, Baltimore, MD, May 2002, pp. 345–349.

[17] B. Scheers, M. Acheroy, A. Vander Vorst, Time-domain simulation and characterization of TEM horns using a normalized impulse response, IEE Proc.-Microw. Antennas Propag. 147 (6) (2000) 463–468.

[18] B. Parr, B. Cho, K. Wallace, Z. Ding, A novel ultra-wideband pulse design algorithm, IEEE Comm. Lett. 7 (5) (2003) 219–221.

[19] L. Bin, E. Gunawan, L.C. Look, On the BER performance of TH-PPM UWB using Parr's monocycle in the AWGN channel, IEEE Conference on Ultra Wideband Systems and Technologies, Reston, VA, November 2003, pp. 403–407.

[20] X. Wu, Z. Tian, T.N. Davidson, G.B. Giannakis, Optimal waveform design for UWB radios, IEEE International Conference on Acoustics, Speech, and Signal Processing, vol. 4, May 2004, pp. 521–524.

[21] H. Sheng, P. Orlik, A.M. Haimovich, L.J. Cimini Jr., J. Zhang, On the spectral and power requirements for ultra wideband transmission, IEEE International Conference on Communications, vol. 1, May 2003, pp. 738–742.

[22] B.P. Crow, I. Widjaja, J.G. Kim, P.T. Sakai, IEEE 802.11: wireless local area networks, IEEE Comm. Mag. 35 (9) (1997) 116–126.

[23] A. Ghosh, D.R. Wolter, J.G. Andrews, R. Chen, Broadband wireless access with WiMax/802.16: current performance benchmarks and future potential, IEEE Comm. Mag. 43 (2) (2005) 129–136.

[24] J.C. Haartsen, The bluetooth radio system, IEEE Personal Comm. 7 (1) (2000) 28–36.

[25] M. Mouly, M.B. Pautet, The GSM System for Mobile Communication, CellSys, 1992.

[26] M. Chiang, Balancing transport and physical layers in wireless multihop networks: jointly optimal congestion control and power control, IEEE J. Selected Areas Comm. 23 (1) (2005) 104–116.

[27] H.E. Rowe, Signals and Noise in Communications Systems, D Van Nostrand Company, Inc., Princeton, New Jersey, 1965.